



Pradeilles, J. A., Zhong, S., Baglyas, M., Tarczay, G., Butts, C. P., Myers, E. L., & Aggarwal, V. K. (2020). Odd–even alternations in helical propensity of a homologous series of hydrocarbons. *Nature Chemistry*, 12, 475-480. <https://doi.org/10.1038/s41557-020-0429-0>

Peer reviewed version

License (if available):
CC BY

Link to published version (if available):
[10.1038/s41557-020-0429-0](https://doi.org/10.1038/s41557-020-0429-0)

[Link to publication record in Explore Bristol Research](#)
PDF-document

This is the author accepted manuscript (AAM). The final published version (version of record) is available online via Nature Research at <https://www.nature.com/articles/s41557-020-0429-0> . Please refer to any applicable terms of use of the publisher.

University of Bristol - Explore Bristol Research

General rights

This document is made available in accordance with publisher policies. Please cite only the published version using the reference above. Full terms of use are available:
<http://www.bristol.ac.uk/red/research-policy/pure/user-guides/ebr-terms/>

Odd–even alternations in helical propensity of a homologous series of hydrocarbons

Johan A. Pradeilles,^{†1} Siying Zhong,^{†1} Márton Baglyas,^{2,3} György Tarczay,^{2,3} Craig P. Butts,^{1*} Eddie L. Myers^{4*} & Varinder K. Aggarwal^{1*}

Abstract

Odd and even homologues of some *n*-alkane-based systems are known to exhibit significantly different trends in solid state properties; a well-known illustration is the zig–zag plot of their melting point versus chain length. Odd–even effects in the solid state often arise from intermolecular interactions involving fully extended molecules. These effects have also been observed in less condensed phases, such as self-assembled monolayers; however, the origins of these effects in such systems can be difficult to determine. Here, combining NMR and computational analysis, we show that all-*syn* contiguously methyl-substituted hydrocarbons, with chain lengths from C6 to C11, exhibit a dramatic odd–even effect in helical propensity. The even- and odd-numbered hydrocarbons populate regular and less controlled helical conformations, respectively. This knowledge will guide the design of helical hydrocarbons as rigid scaffolds or as hydrophobic components in soft materials.

[†]These authors contributed equally to this work. ¹School of Chemistry, University of Bristol, Cantock's Close, Bristol BS8 1TS, UK. ²Laboratory of Molecular Spectroscopy, Institute of Chemistry, Eötvös University, PO Box 32, H-1518, Budapest 112, Hungary. ³MTA-ELTE, Lendület Laboratory Astrochemistry Research Group, Institute of Chemistry, Eötvös University, PO Box 32, H-1518, Budapest 112, Hungary. ⁴School of Chemistry, NUI Galway, University Road, Galway, Ireland. *e-mail: v.aggarwal@bristol.ac.uk; eddie.myers@nuigalway.ie; craig.butts@bristol.ac.uk

In 1887, Baeyer discovered that *n*-alkyl carboxylic acids do not undergo a monotonic increase in melting point with increasing chain length.¹ Instead, the series of molecules containing an even number of carbon atoms tended to have higher melting points than the series containing an odd number of carbon atoms (**Figure 1a**). X-ray crystallographic analysis later confirmed that the origin of this odd–even effect was that the even series had optimal intermolecular interactions of their termini when packed together in their fully-extended zig–zag conformer.^{2,3} Since then, odd–even effects in other bulk properties of *n*-alkane-based systems have been well documented and studied.⁴ Some of the most intriguing odd–even effects are those associated with the properties of self-assembled monolayers (SAMs) of *n*-alkanethiols on metal surfaces (**Figure 1b**). Although these odd–even effects, which reveal themselves in surface-wetting properties^{4,5} and current densities of molecular junctions,^{6,7} can have significant technological implications, the origin of each effect remains poorly understood. Some have been linked to the solid-like characteristics of these semi-condensed phases; for example, in the fully extended zig–zag arrangement, the odd and even systems exhibit different orientations of the free-end terminal groups, which interface differently with wetting liquids⁵ or, in the case of molecular junctions, with the top electrode.⁶ However, recently, odd–even effects have been linked to the liquid-like characteristics of self-assembled monolayers, specifically, the level of deviation of chains from the all-*trans* conformer to so called ‘*gauche* defect’ conformers, dynamic behaviour that appears to alternate in a zig–zag fashion with increasing chain length.^{8,9,10} Furthermore, molecular dynamics simulations predict odd–even effects in the stretch-induced coil–to–helix transition of isotactic polypropylenes.¹¹ Here we show a rare manifestation of the odd–even effect in the conformational behaviour of all-*syn* contiguously methyl-substituted hydrocarbons, which are useful systems for the study and exploitation of helical conformers of hydrocarbons and display marked odd–even effects in their propensity to form regular helical conformers.

Using iterative stereodefined homologation of boronic ester-terminated hydrocarbons (**Figure 2a**), a process termed lithiation–borylation, which has been recently developed in our laboratory,¹² we have prepared conformationally defined contiguously methyl-substituted hydrocarbons as single enantiomers. These molecules exhibit different shapes, linear (**Figure 2b**) or helical (**Figure 2c**), depending on the relative configuration of the methyl groups, thus providing access to molecular systems that can be used to both probe and exploit specific subsets of the many conformers that are accessible in the more flexible parent *n*-alkanes.¹³ Supported by exhaustive computational modelling and NMR analysis, we proved that the disyndiotactic (alternating *syn–anti*) isomer **7** heavily populated a fully extended zig–zag conformer (linear) in solution, while the corresponding *threo*-diisotactic (all-*syn*) isomer **8** heavily populated a helical conformer.¹³

This result is consistent with and can be understood by using theoretical analysis that was put forward by Hoffmann in the 1990s.¹⁴ He articulated a useful description of the conformation of hydrocarbons as being defined by a sequence of dihedral angles involving the carbon atoms of the principal chain, with the terms g^+ , g^- and t , denoting dihedral angles of approximately $+60^\circ$, -60° and 180° , respectively. For methyl-substituted hydrocarbons, when a g^+ dihedral angle is immediately followed by a g^- dihedral angle, two carbon units (four bonds apart from each other) are brought to within about 2.5 Å. This destabilising $g^+ g^-$ interaction, commonly called a *syn*-pentane interaction (**Figure 2d**), is worth ca. 3.3–3.7 kcal mol⁻¹.¹⁵ To avoid these interactions, all-*syn* and *syn–anti* contiguously methyl-substituted hydrocarbons adopt alternating $g^+ t$ (or $g^- t$) and all- t dihedral angles, which describe their helical and linear shapes, respectively.

The (*S,R,S,R,S,S,R,S,R,S*) enantiomer of an all-*syn* isomer with hydroxyl and biphenyl terminal groups (**8**) adopted an *M* helix in solution, while its crystalline benzoate derivative (**9**) adopted a *P* helix in the solid state.¹³ This result showed that both *P* and *M* helical forms were accessible to the molecule and although one helical form was favoured in solution, this preference could be over-ridden by crystal packing forces in the solid state. Intrigued by this observation, we wished to understand the origin of the sense of helicity, particularly in solution. In this work, we therefore initiated a computational and experimental investigation to establish the relationship between the structure and the sense of helicity of all-*syn* methyl-substituted hydrocarbons, thereby building a theoretical framework from which technological applications in catalysis, materials, and medicine could emerge.

Results and discussion

We decided to base our study on the **C6–C11** series of all-*syn* contiguously methyl-substituted hydrocarbons with alkyne groups at the termini (**Figure 3d**). The terminal alkyne groups were deemed suitably non-imposing to allow the methine units to dominate the control of structural order. Overlaying the **C10** isomer onto the idealised diamond-lattice template revealed that only two conformers could avoid *syn*-pentane interactions, namely an *M* (left-handed) helix and a *P* (right-handed) helix (**Figure 3a**). Following Hoffmann's notation, their dihedral angle sequences are $t g^+ t g^+ t g^+ t g^+ t$ and $g^- t g^- t g^- t g^- t g^-$, respectively. The corresponding Newman projections show that each *t* (180°) dihedral angle creates 3 *gauche* interactions while each *g* (±60°) dihedral angle generates only 2 *gauche* interactions (**Figure 3c**). To reduce the number of steric interactions, the molecule would be expected to adopt a conformer that maximises the number of *g* dihedral angles and minimises the number of *t* dihedral angles. Therefore, this qualitative analysis would predict that **C10** would adopt a right-handed helix (22 *gauche* interactions) in preference to a left-handed helix (23 *gauche*

interactions), as would other homologues in the same enantiomeric series that contain an even number of methines. For homologues containing an odd number of methine units, such as **C11**, which is achiral (*meso*) owing to the mirror plane containing the central carbon atom and its methyl substituent, both *M* and *P* helices contain 25 *gauche* interactions, with *g* and *t* dihedral angles at opposing termini (**Figure 3b**). Therefore, for odd systems one would predict a 1:1 mixture of *M* and *P* helices with a high degree of regularity. To confirm these predictions, a detailed computational investigation of the conformational behaviour of these molecules were undertaken.

A molecular mechanics conformational search of **C10** found 45 conformers, which were subjected to density functional theory (DFT) geometry optimisation and free-energy calculations. These DFT calculations confirmed that **C10** has a strong preference for helical conformers, which constitute 79% of the total population (**Figure 4b**). Of these helical conformers, which exhibit a narrow range of pitch values, 82% are *P* helices ($g^- t g^- t g^- t g^- t g^-$; 22 *gauche* interactions) and 18% are *M* helices ($t g^+ t g^+ t g^+ t g^+ t$; 23 *gauche* interactions), a diastereomeric ratio that is consistent with the extra *gauche* interaction (ca. 1 kcal mol⁻¹) in *M* helices.¹⁵ The same computational analysis was performed on the shorter homologues, **C6** and **C8**, confirming that the corresponding *P* and *M* helices, respectively, are the preferred conformers in solution, the sense of helicity following the absolute configuration of the enantiomeric series of homologues to which they belong. The **C6** and **C8** compounds have a strong conformational preference for fully helical conformers, the populations registering 86% and 80%, respectively (**Figure 3e**). The overall drop in helical population with increasing chain length is in line with the increasing entropic cost of adopting defined conformers as the number of freely rotatable bonds increases.¹⁶ The calculated difference in energy between the *M* and *P* helices for both the **C6** and **C8** compounds is ca. ± 1 kcal mol⁻¹,

which is similar to the value calculated for **C10**. Overall, the **C6**, **C8** and **C10** hydrocarbons preferentially adopt helical conformers that present *g* dihedral angles at the termini (*g*[−] for **C6/C10** and *g*⁺ for **C8**), thus minimising the overall number of *gauche* interactions.

Computational analysis of *meso* (and odd-numbered) homologues **C7**, **C9** and **C11** revealed, as predicted, a 1:1 mixture of *M* and *P* helices.¹⁷ However, the shortest member of this series, **C7**, exhibits only a moderate preference for entirely helical conformers, a preference that quickly vanishes upon increasing the length (**C7**: 63%, **C9**: 49%, **C11**: 27%; **Figure 3e**). Closer analysis of **C11** revealed that in the helical conformers, which were present in a low population (27%), one end-group adopts a low-energy *gauche* orientation with respect to the main chain, the other adopting the high-energy *trans* orientation. However, in most non-helical conformers, both terminal end-groups adopt the low-energy *gauche* orientation, facilitated through the introduction of a kink¹⁸ (or relaxed *syn*-pentane interaction) in the chain. Consequently, for these odd-numbered hydrocarbons, the helical conformers (with one end-group necessarily in the costly *trans* orientation) and non-helical conformers (with a relaxed *syn*-pentane interaction in the chain) are very close in energy (<1 kcal mol^{−1}; cf. 1.7–1.8 kcal mol^{−1} for **C6/C8/C10**), the degeneracy suppressing control over the degree of helicity.

Overall, DFT calculations predict that for compounds with an even number of methines, such as **C10**, the lowest-energy conformer, which is helical, presents both end-groups in a *gauche* relationship with the main chain. Here, both end-groups, which are substituents on carbon atoms of the same absolute configuration, induce the same sense of helicity, the reinforcement leading to control over the degree of helicity, which is only relinquished gradually by the entropic cost of increasing chain length (**Figure 3d,e**). The alternating preference for *P* and *M*

helices is dictated by the absolute configuration of the end groups, which alternates from *R* to *S* as chain length increases bidirectionally. For compounds with an odd number of methines in the main chain (*meso* homologues), such as **C11**, the end-groups are substituents on carbon atoms of opposite absolute configuration. The end-groups will only induce the same sense of helicity when one end-group is placed in a *gauche* relationship with the main chain while the other is in a higher energy *trans* relationship. When both end-groups are placed in the low-energy *gauche* relationship with the main chain, they induce the opposite sense of helicity, thus creating a kink in the chain. These internally defective helical conformers are very similar in energy to the purely helical conformers, which necessarily present *gauche*- and *trans*-orientated end-groups. With increasing length, the number of positions where the defect can present itself also increases, the increasing degeneracy leading to a rapid drop in overall control of helical character (**Figure 3d,e**).

With the above predictions in hand, we needed to synthesise these molecules and examine their behaviour in solution to validate our theoretical expectations. Our group previously reported methodology¹³ for the iterative homologation of boronic esters to synthesise compounds like **C10**. The protocol (**Figure 2a**) involved subjecting a suitable starting pinacol boronic ester to an iterative two-step process involving (i) the formation of a boronate complex (**3**) by adding the pinacol boronic ester (**1**) to a solution of a configurationally-stable enantioenriched methyl-substituted lithium carbenoid (**2**) at low temperature, and (ii) the stereospecific 1,2-metallate rearrangement of this boronate complex, which was promoted at higher temperature, to deliver the one-carbon extended boronic ester. Owing to the C_2 symmetry of carbon chains that contain an even number of methine units, such as **C10**, we decided to investigate a bidirectional homologation of a bis(boronic ester), thus cutting the number of synthetic steps in half compared to the unidirectional strategy. At the end of the

growth phase, the terminal boronic esters could then be stereospecifically converted into alkyne groups, by using a methodology developed earlier in our group.¹⁹

Rhodium-catalysed asymmetric diboration^{20,21} of *trans*-butene (**12**) provided the requisite starting bis(boronic ester) (**Figure 4a**). Although 2,3-bis(boronic ester) **13a** was obtained in high enantioselectivity (>99.5:0.5 *e.r.*) and high diastereoselectivity (>95:5 *d.r.*), it could not be separated from the 1,2-substituted regioisomer arising from initial alkene isomerisation. Pleasingly, however, after the first round of bidirectional double homologation, bis(boronic ester) **14** could be purified by recrystallisation to provide chemically and enantiomerically pure material for further homologation. At this stage, an X-ray structure confirmed the relative configuration of the four stereogenic centres. Bis(boronic ester) **14** was subjected to three further iterations of double homologations, switching the enantiomer of the lithium carbenoid used at each iteration, to deliver all-*syn* bis(boronic ester) **18**, which could be successfully converted into bis(alkyne) **C10** by using our recently developed stereospecific alkynylation methodology.¹⁹ Target molecules **C6** and **C8** were obtained from the same protocol, through terminating the sequence after the second and third iterations of homologation, respectively. Notably, the use of the same bidirectional protocol for generating **C6**, **C8** and **C10** has the consequence that it delivers **C6/C10** and **C8** as homologues of opposing enantiomeric series (**C6/C10** have *R*-configured terminal methine units, **C8** has *S*-configured terminal methine units); a common unidirectional approach would lead to **C6**, **C8** and **C10** being part of the same enantiomeric series. The *meso* homologues **C7**, **C9** and **C11** were prepared from the bis(boronic ester) derivatives of **C6**, **C8** and **C10**, respectively, through careful alkynylation of one of the equivalent terminal boryl groups, protection of the resulting terminal alkyne as the triisopropylsilyl derivative, homologation of the remaining boronic ester with the requisite enantiomer of the lithium carbenoid, alkynylation and

deprotection (**Figure 4g**). With target molecules **C6–C11** in hand, their conformational behaviour in solution was then investigated by using a comparison of their computed conformers, populations and NMR parameters with experimental solution-state NMR spectroscopic data. In line with the predicted levels of conformational control, compound **C10** was a crystalline solid (m.p. 88–92 °C), whereas **C11** was a liquid at room temperature, demonstrating how one additional carbon can be the difference between order and chaos.

The DFT-calculated ^1H – ^1H scalar coupling constants and interproton distances that would be derived from nuclear Overhauser effect (nOe) measurements for **C6**, **C8** and **C10** (each averaged across their calculated population of conformers) were compared to the experimentally measured values (**Figure 4c**). The resulting goodness of fit is in line with that observed for conformational analysis of compounds of similar structural complexity^{11,13} and reflects their relatively high conformational control (^1H – ^1H coupling: mean absolute deviation (MAD) = 0.1–0.5 Hz, standard deviation (StDev) = 0.1–0.5 Hz; nOe distances: MAD = 2.9–4.2%, StDev = 1.8–5.4%). The experimentally acquired vibrational circular dichroism (VCD) spectrum of **C10** in CDCl_3 was a close match to the DFT-predicted simulation for the **C10** *P* helix (**Figure 4f**), thus in agreement with the predicted sense and level of helical chirality (ca. *P/M* 90:10). Additionally, more intense VCD signals are observed at lower temperature supports the assertion that the slight drop in helicity across the even series is due to the increased entropic cost of retaining full helicity upon chain elongation (**Supplementary Figure 7b**). A selection of alternative **C10** molecules with other terminal groups (1-naphthyl, **31**; hydroxy, **32**; acetoxy, **33**; amino, **35** and dibenzylamino, **36**), prepared through stereospecific transformations of the intermediate bis(boronic ester) **18** and analysed as described above, all adopted the expected *P* helix in solution. Comparable analysis for the less-controlled odd members of the series also supports the DFT-predicted levels of helical

control. **C7** provides a good fit to NMR experimental results (^1H – ^1H coupling: MAD = 0.3 Hz, StDev = 0.2 Hz; nOe distances: MAD = 4.1%, StDev = 6.0%). Notably, fitting the experimental nOe data to only a 1:1 mixture of *M* and *P* helices (**Supplementary Table 22**) provides a notably worse fit, demonstrating that non-helical conformers are indeed present in solution. **C9** and **C11** give similar outcomes (^1H – ^1H coupling: MAD = 0.3–1.0 Hz, StDev = 0.3–1.4 Hz; nOe distances: MAD = 5.4–6.7%, StDev = 6.5–8.9%) with the quality of fit falling off as the chain is extended to **C11** in line with the population estimates by DFT becoming more sensitive to the increased number of low energy non-helical conformers possible in this more complex conformational landscape.

Conclusions

Our experimental and computational studies on all-*syn* contiguously methyl-substituted hydrocarbons have revealed a rare odd–even effect in alkanes that is not associated with bulk intermolecular interactions.^{22,23} For future technological applications, these fundamental findings will guide the design of molecules with desirable conformational, and thus physicochemical, properties. Carbon chains with an even number of methine groups will lead to molecules with well-defined helical conformers for their application as non-switchable rigid materials or as scaffolds for the presentation of molecular recognition elements. Carbon chains with an odd number of methine groups, although adopting less regular conformations with identical terminal groups, provide more ready access to both *M* and *P* helical forms, offering the potential to manipulate their conformational landscape through judicious end-group selection. Through covalent or non-covalent modification of end-groups, the conformational landscape could be switched from one screw-sense to another for applications in materials. Furthermore, these results highlight the potentially important role of dynamic behaviour in the origin of bulk odd–even effects in condensed phases, a connection that has

recently been proposed for explaining trends in some properties of liquids²⁴ and self-assembled monolayers.^{8,25}

Data availability

Crystallographic data for the structures reported in this Article have been deposited at the Cambridge Crystallographic Data Centre, under deposition numbers CCDC 1908685 (**14**), 1908684 (**18**), 1908686 (**C10**), 1935492 (**31**), 1935491 (**32**) and 1935490 (**36**). Copies of the data can be obtained free of charge via <https://www.ccdc.cam.ac.uk/structures/>. All other data supporting the findings of this study are available within the Article and its Supplementary Information, or from the corresponding author upon reasonable request.

Code availability

The Python script used in the computational study is included in the Supporting Information file.

References

- 1 Baeyer, A. Ueber Regelmässigkeiten im Schmelzpunkt homologer Verbindungen. *Berichte der Dtsch. Chem. Gesellschaft* **10**, 1286–1288 (1877).
- 2 Boese, R., Weiss, H.-C. & Bläser, D. The Melting Point Alternation in the Short-Chain *n*-Alkanes: Single-Crystal X-Ray Analyses of Propane at 30 K and of *n*-Butane to *n*-Nonane at 90 K. *Angew. Chem. Int. Ed.* **38**, 988–992 (1999).
- 3 Bond, A. D. On the crystal structures and melting point alternation of the *n*-alkyl carboxylic acids. *New J. Chem.* **28**, 104–114 (2004).

- 4 Tao, F. & Bernasek, S. L. Understanding Odd–Even Effects in Organic Self-Assembled Monolayers. *Chem. Rev.* **107**, 1408–1453 (2007).
- 5 Newcomb, L. B. *et al.* Odd–Even Effect in the Hydrophobicity of *n*-Alkanethiolate Self-Assembled Monolayers Depends upon the Roughness of the Substrate and the Orientation of the Terminal Moiety. *Langmuir* **30**, 11985–11992 (2014).
- 6 Baghbanzadeh, M. *et al.* Odd–Even Effects in Charge Transport across *n*-Alkanethiolate-Based SAMs. *J. Am. Chem. Soc.* **136**, 16919–16925 (2014).
- 7 Jiang, L., Sangeeth, C. S. S. & Nijhuis, C. A. The Origin of the Odd–Even Effect in the Tunneling Rates across EGaIn Junctions with Self-Assembled Monolayers (SAMs) of *n*-Alkanethiolates. *J. Am. Chem. Soc.* **137**, 10659–10667 (2015).
- 8 Chen, J., Chang, B., Oyola-Reynoso, S., Wang, Z. & Thuo, M. Quantifying *Gauche* Defects and Phase Evolution in Self-Assembled Monolayers through Sessile Drops. *ACS Omega* **2**, 2072–2084 (2017).
- 9 Ramin, L. & Jabbarzadeh, A. Odd–Even Effects on the Structure, Stability, and Phase Transition of Alkanethiol Self-Assembled Monolayers. *Langmuir* **27**, 9748–9759 (2011).
- 10 Chen, J. *et al.* Understanding Interface (Odd–Even) Effects in charge tunneling using a polished EGaIn electrode. *Phys. Chem. Chem. Phys.* **20**, 4864–4878 (2018).

- 11 Xie, C., Tang, X., Yang, J., Xu, T., Tian, F. & Li, L. Stretch-Induced Coil–Helix Transition in Isotactic Polypropylene: A Molecular Dynamics Simulation. *Macromolecules* **51**, 3994–4002 (2018).
- 12 Stymiest, J. L., Dutheuil, G., Mahmood, A. & Aggarwal, V. K. Lithiated Carbamates: Chiral Carbenoids for Iterative Homologation of Boranes and Boronic Esters. *Angew. Chem. Int. Ed.* **46**, 7491–7494 (2007).
- 13 Burns, M. *et al.* Assembly-line synthesis of organic molecules with tailored shapes. *Nature* **513**, 183–188 (2014).
- 14 Hoffmann, R. W. Flexible Molecules with Defined Shape—Conformational Design. *Angew. Chem. Int. Ed.* **31**, 1124–1134 (1992).
- 15 Tsuzuki, S. *et al.* Investigation of Intramolecular Interactions in *n*-Alkanes. Cooperative Energy Increments Associated with GG and GTG' Sequences . *J. Am. Chem. Soc.* **113**, 4665–4671 (1991).
- 16 Hoffmann, R. W., Stahl, M., Schopfer, U. & Frenking, G. Conformation Design of Hydrocarbon Backbones: A Modular Approach. *Chem. - A Eur. J.* **4**, 559–566 (1998).
- 17 Wechsel, R., Raftery, J., Cavagnat, D., Guichard, G. & Clayden, J. The *meso* Helix: Symmetry and Symmetry-Breaking in Dynamic Foldamers with Reversible Hydrogen-Bond Polarity. *Angew. Chem. Int. Ed.* **55**, 9657–9661 (2016).

- 18 Tomsett, M. *et al.* A tendril perversion in a helical oligomer: trapping and characterizing a mobile screw-sense reversal. *Chem. Sci.*, **8**, 3007–3018 (2017).
- 19 Wang, Y., Noble, A., Myers, E. L. & Aggarwal, V. K. Enantiospecific Alkynylation of Alkylboronic Esters. *Angew. Chem. Int. Ed.* **55**, 4270–4274 (2016).
- 20 Morgan, J. B., Miller, S. P. & Morken, J. P. Rhodium-Catalyzed Enantioselective Diboration of Simple Alkenes. *J. Am. Chem. Soc.* **125**, 8702–8703 (2003).
- 21 Trudeau, S., Morgan, J. B., Shrestha, M. & Morken, J. P. Rh-Catalyzed Enantioselective Diboration of Simple Alkenes: Reaction Development and Substrate Scope. *J. Org. Chem.* **70**, 9538–9544 (2005).
- 22 Izumi, H., Yamagami, S., Futamura, S., Nafie, L. A. & Dukor, R. K. Direct Observation of Odd–Even Effect for Chiral Alkyl Alcohols in Solution Using Vibrational Circular Dichroism Spectroscopy. *J. Am. Chem. Soc.* **126**, 194–198 (2004).
- 23 Lüttschwager, N. O. B., Wassermann, T. N., Mata, R. A. & Suhm, M. A. The Last Globally Stable Extended Alkane. *Angew. Chem. Int. Ed.* **52**, 463–466 (2013).
- 24 Yang, K. *et al.* Dynamic Odd–Even Effect in Liquid *n*-Alkanes near Their Melting Points. *Angew. Chem. Int. Ed.* **55**, 14090–14095 (2016).

25 Liu, B. *et al.* Polyfluorene (PF) Single-Chain Conformation, β Conformation, and Its Stability and Chain Aggregation by Side-Chain Length Change in the Solution Dynamic Process. *J. Phys. Chem. C* **122**, 14814–14826 (2018).

Acknowledgements

We thank H2020 ERC (670668) for financial support. We thank Natalie Pridmore and Hazel Sparkes for assistance with X-ray analysis, Matthew Davey for useful discussions about VCD and William Gerrard for his contribution to data processing. S.Z. thanks the EPSRC Bristol Chemical Synthesis Doctoral Training Centre for a studentship (EP/L015366/1). We thank Szilárd Varga (Hungarian Academy of Sciences Research Centre for Natural Sciences) for supporting the VCD measurements. The work at Eötvös University was completed within the framework of the ELTE Excellence Program (1783-3/2018/FEKUTSTRAT) supported by the Hungarian Ministry of Human Capacities (EMMI).

Author Contributions

J.P. and S.Z. contributed equally to this work. V.K.A., C.P.B. and E.L.M. designed the project. J.A.P. conducted and designed the experiments and analysed the data. S.Z. conducted and designed the computational studies and NMR experiments. M.B. and G.T. performed the VCD experiments and analysed the data. J.A.P., S.Z., E.L.M., C.P.B. and V.K.A. wrote the manuscript.

Competing interests

The authors declare no competing interests.

Additional information

Supplementary information is available for this paper at <https://doi.org/xx.xxxx/xxxxxxx-xxx-xxxx-x>.

Reprints and permissions information is available online at www.nature.com/reprints.

Correspondence and requests for materials should be addressed to V.K.A., E.L.M. or C.P.B.

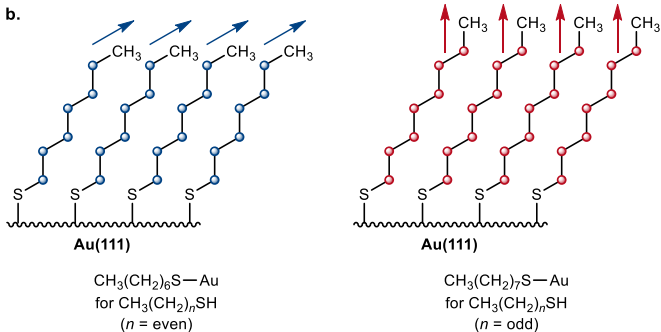
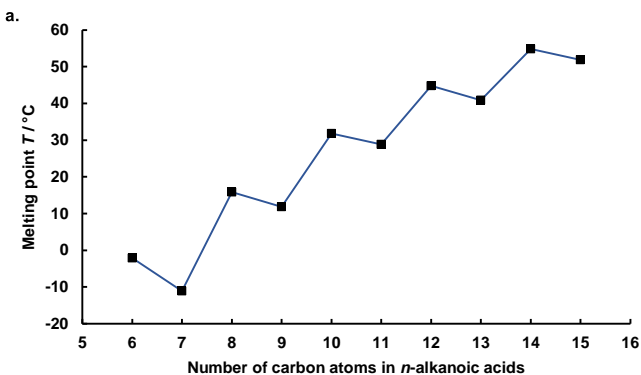
Figure 1. Known examples of odd–even effects associated with bulk properties. **a.** Graph showing effect of chain length on the melting point of a series of *n*-alkyl carboxylic acids, demonstrating a zig–zag rather than a monotonic increase in melting point as the chain length increases. **b.** The orientation of the terminal methyl groups of self-assembled *n*-alkanethiolate monolayers on Au(111) is known to depend on whether there is an odd or an even number of carbon atoms in the chain. Blue and red dots represent CH₂ groups in an odd-numbered and even-numbered *n*-alkanethiolate carbon chain, respectively.

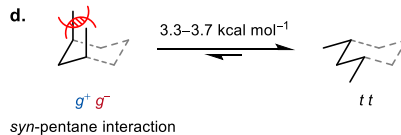
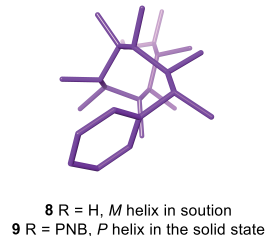
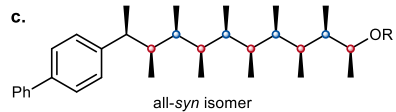
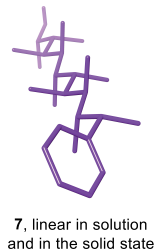
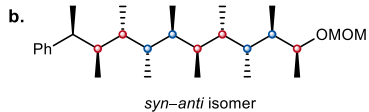
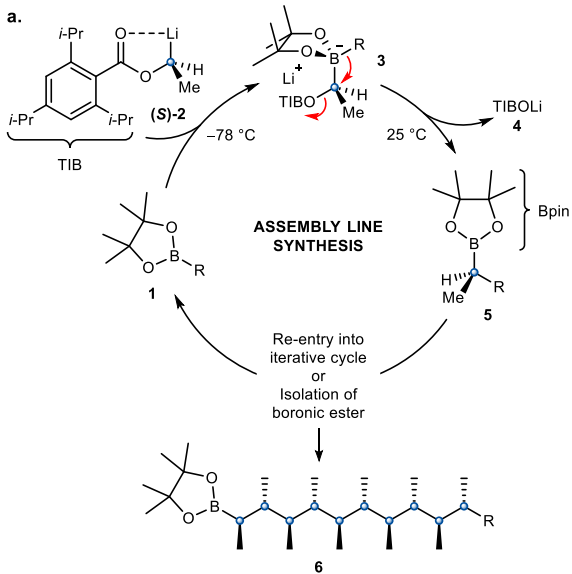
Figure 2. Previously-reported iterative homologation of boronic esters and conformational control.¹³ **a.** Reagent-controlled iterative homologations of boronic esters is employed for the rapid synthesis of stereodefined methyl-substituted carbon chains. **b.** The alternating *syn–anti* isomer adopts an extended linear shape in solution and in the solid state to avoid *syn*–pentane interactions. **c.** The all-*syn* isomers **8** and **9** fold into a left-handed (*M*) helix in solution and a right-handed (*P*) helix in the solid state, respectively, to avoid *syn*–pentane interactions. **d.** The conformation of such molecules is controlled through the avoidance of *syn*–pentane interactions.

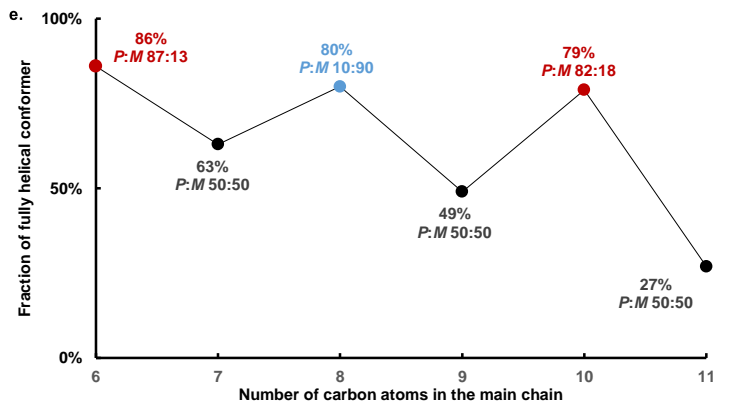
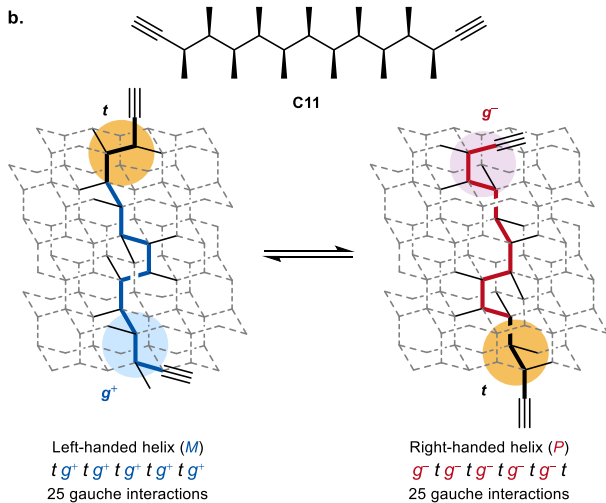
Figure 3. Relationships between chain length, sequence of dihedral angles and conformational behaviour. **a.** Even-numbered carbon chains preferentially adopt the helical conformer with *g* dihedral angles at both termini, thus reducing the number of *gauche* interactions in the molecule. The terms *g*⁺, *g*[–] and *t* denote dihedral angles of approximately +60°, –60° and 180°, respectively. **b.** To fold into a helix, odd-numbered carbon chains must have one *t* and one *g* terminal dihedral angle. Both helical conformers present the same number of *gauche* interactions. **c.** Any *t* dihedral angle generates 3 *gauche* interactions whereas any *g* dihedral angle creates only 2 *gauche* interactions. **d.** The preference of the

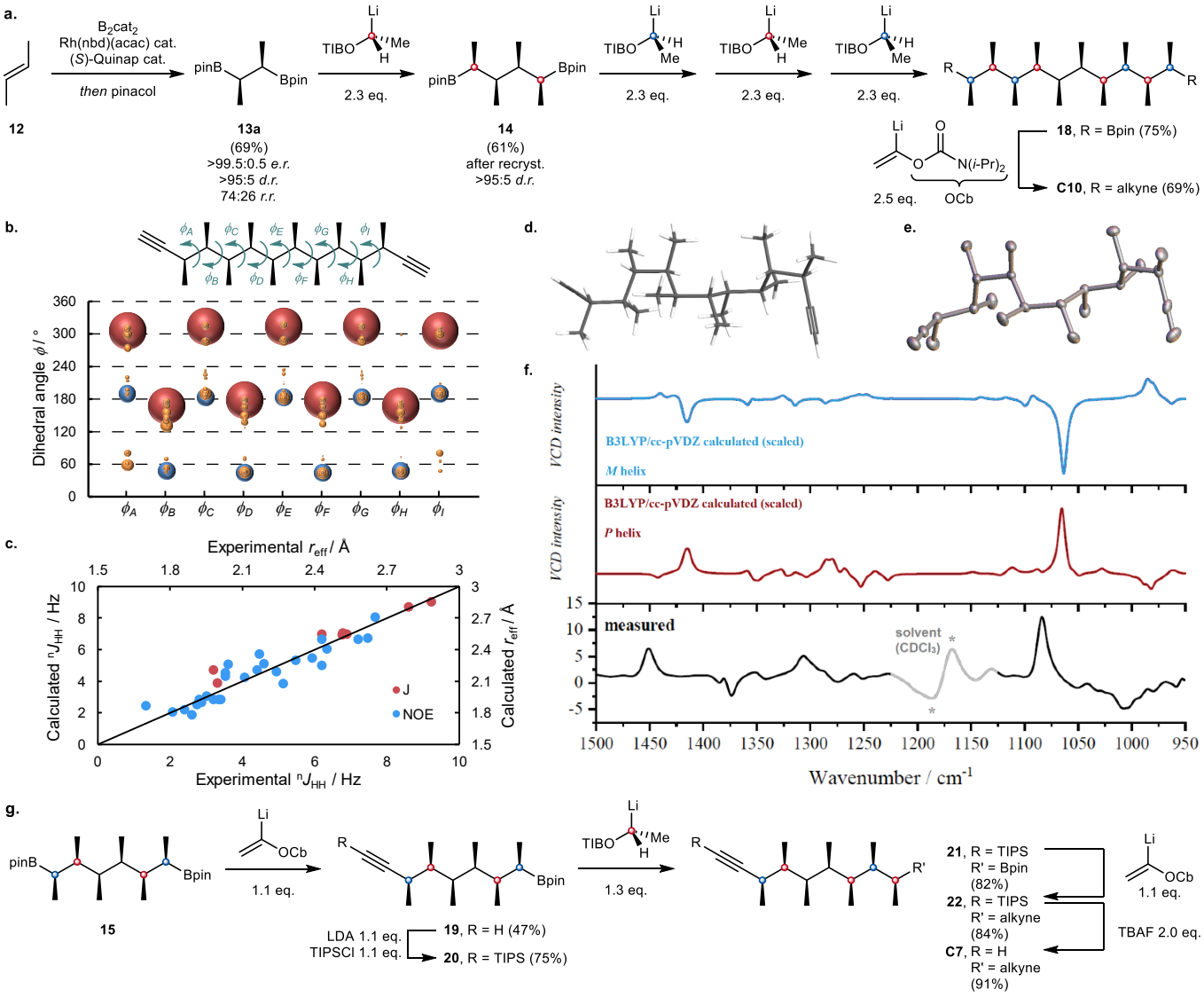
termini to present a sterically-favoured *g* dihedral angle leads to the even-numbered carbon chains strongly favouring a helical conformation (both termini inducing the same screw-sense) but creates a conflict in the odd-numbered carbon chains, forcing them to adopt less regular conformations. **e.** Graph showing effect of chain length on the helical fraction of all-*syn* methyl-substituted hydrocarbons. An odd–even effect is observed where the helicity of even-numbered hydrocarbons is well controlled but odd-numbered hydrocarbons are less well controlled.

Figure 4. Synthesis and conformational analysis. **a.** Preparation of **C10** using bidirectional assembly-line synthesis. **b.** DFT-derived dihedral angle populations of **C10** represented as a bubble plot. The size of the bubble is proportional to the calculated Boltzmann-averaged population of that conformer. **c.** Correlation between the calculated and the experimentally-determined NMR parameters of **C10**. Purple dots represent the comparison of ^1H – ^1H scalar coupling constants while blue dots represent the comparison of nOe-derived interproton distances. **d.** DFT-predicted lowest energy conformer of **C10**. **e.** X-ray crystal structure of **C10**. Ellipsoids shown at 50% probability. Hydrogen atoms have been omitted for clarity. **f.** Comparison between the calculated VCD spectrum of the lowest energy *M*-helical conformer of **C10** (blue), the calculated VCD spectrum of the lowest *P*-helical conformer of **C10** (red) and the measured VCD spectrum of **C10** (black). This comparison shows that **C10** adopts a *P*-helix in solution. The peaks between $1125\text{--}1225\text{ cm}^{-1}$ (*) are due to interacting solvent (CDCl_3). **g.** Method for the synthesis of odd-numbered compounds, illustrated here for **C7**.

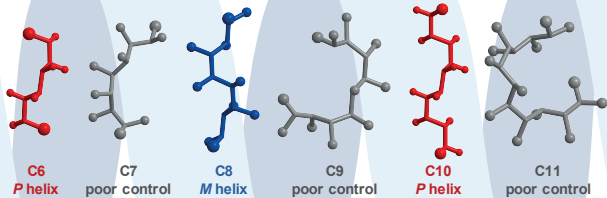








CHAIN LENGTH



CONFORMATIONAL CONTROL